Atmospheric Pollution Research 9 (2018) 494–501

HOSTED BY

Contents lists available at ScienceDirect

Atmospheric Pollution Research

journal homepage: www.elsevier.com/locate/apr

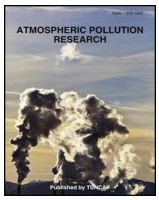

Light absorption characteristics of brown carbon during foggy and non-foggy episodes over the Indo-Gangetic Plain



Vikram Choudhary[a,b], Prashant Rajput[a,*], Dharmendra Kumar Singh[a,c], Amit Kumar Singh[a], Tarun Gupta[a,b]

[a] Department of Civil Engineering and APTL at Center for Environmental Science and Engineering (CESE), Indian Institute of Technology Kanpur, Kanpur 208 016, India
[b] Environmental Engineering and Management Program, Indian Institute of Technology Kanpur, Kanpur 208 016, India
[c] NUS Environmental Research Institute (NERI), National University of Singapore, #02-01, T-Lab Building 5A Engineering Drive 1, Singapore 117 411, Singapore

ARTICLE INFO

Keywords:
Fog-processing
Brown carbon
Mass absorption efficiency
Absorption Ångström exponent
Direct radiative forcing
IGP

ABSTRACT

Atmospheric PM_1 (particulate matter with aerodynamic diameter ≤ 1 μm) samples have been collected during foggy (n = 17) and non-foggy nights (n = 19) in wintertime at Kanpur in central Indo-Gangetic Plain (IGP) to assess light absorption characteristics and direct radiative forcing of water-extractable brown carbon (BrC). We have observed a significant enhancement (two-tailed *t*-test: t = 2.2; at significance level: p < 0.05) in the absorption coefficient of water-extractable BrC at 365 nm ($b_{abs\text{-}BrC\text{-}365}$) from non-foggy (Avg.: 53.5 Mm^{-1}) to foggy episodes (69.3 Mm^{-1}). Enhancement in mass absorption efficiency (MAE) of BrC (1.8 m^2/g C) during foggy episodes is consistent with that of $b_{abs\text{-}BrC\text{-}365}$. Absorption Ångström exponent (AAE) remained similar (2.8) during foggy and non-foggy episodes. Significantly lower value of AAE (2.8) at Kanpur compared to other places in IGP (~5) highlights more light absorbing potential of atmospheric BrC over central IGP. Furthermore, MAE of EC at 660 nm during foggy period (8.5 m^2/g) is relatively high as compared to that during the non-foggy episode (7.0 m^2/g). The MAE of BrC and EC exhibited enhancement by ~15% and 20%, respectively during foggy events. These observations are also reflected by an increase (t = 11.1; p < 0.05) in direct radiative forcing of water-extractable BrC (relative to EC) in the atmosphere: from 23.7 ± 10.8% during non-foggy to 54.3 ± 16.5% during foggy episodes. Differences in chemical composition, loading, absorption properties and direct radiative forcing (DRF) of carbonaceous aerosols during non-foggy and foggy episodes indicate predominant influence of fog-processing.

1. Introduction

Carbonaceous aerosols constitute a dominant fraction of fine-particulate matter (Artaxo et al., 2002; Rajput et al., 2018; Rengarajan et al., 2007). It is broadly comprised of black carbon and a large suit of organic aerosols (Gustafsson et al., 2009; Pavuluri et al., 2011; Rajput et al., 2014b; Singh and Gupta, 2015, 2016). Black carbon exhibits strong absorption in visible solar spectrum (Ram and Sarin, 2009; Ram et al., 2012; Singh et al., 2014). Some of the organic species show solar absorption behavior in UV and near-blue region (300–400 nm) (Andreae and Gelencser, 2006; Chen and Bond, 2010; Cheng et al., 2011, 2016; Choudhary et al., 2017; Hecobian et al., 2010). The light absorbing component of organic aerosols is widely referred to as brown carbon (BrC). Several studies on BrC characterization in ambient aerosols have attributed its major sources to primary emission from biomass burning, fossil-fuel combustion and also from secondary transformations (Hoffer et al., 2004; Lack et al., 2013; Lukács et al., 2007; Zheng et al., 2013). Experiments on biomass burning emission characterization during LBA – SMOCC (Large scale Biosphere atmosphere experiment in Amazonia – SMOke aerosols, Clouds, rainfall and Climate) have shown that absorption behavior of humic like substances (HULIS) look similar to that of organic carbon extractable in water (water-soluble organic carbon: WSOC) (Hoffer et al., 2004, 2006). Furthermore, these studies have revealed that BrC derived from biomass burning emission is predominantly comprised of HULIS (Kumar et al., 2017). In this context, it is important to mention that during wintertime the Indo-Gangetic Plain (IGP) experiences massive emissions of carbonaceous aerosols from biomass burning (Rajput et al., 2014b; Ramanathan and Carmichael, 2008). High content of moisture resulting from westerly disturbances, low ambient temperature and shallower planetary boundary layer height causes prolonged fog and haze episodes over this region during wintertime (Chakraborty et al.,

Peer review under responsibility of Turkish National Committee for Air Pollution Research and Control.
* Corresponding author.
E-mail address: prajput@iitk.ac.in (P. Rajput).

https://doi.org/10.1016/j.apr.2017.11.012
Received 2 October 2017; Received in revised form 21 November 2017; Accepted 25 November 2017
Available online 06 December 2017
1309-1042/ © 2018 Turkish National Committee for Air Pollution Research and Control. Production and hosting by Elsevier B.V.

2017; Rajput et al., 2018). It has been emphasized earlier that a detailed understanding on light-absorption properties of BrC from different geographical locations is of utmost importance for assessing its impact on climate forcing (Park et al., 2010).

Challenges in estimating direct radiative forcing due to BrC on a global scale are largely due to high variability in their optical properties (Choudhary et al., 2017; Lee et al., 2014; Massabò et al., 2016). High variability in absorption properties of BrC has been attributed to its source/formation pathway, combustion condition etc. (Saleh et al., 2014; Satish et al., 2017). The BrC aerosols exhibit complex composition (contain myriads of compounds), and thus, their exact quantification is not feasible with current state of analytical techniques. Hence, WSOC and OC are generally used as surrogates for water extractable BrC and methanol extractable BrC, respectively (Cheng et al., 2011, 2017; Choudhary et al., 2017; Hecobian et al., 2010; Satish et al., 2017; Srinivas et al., 2016). In this context, a previous study has reported that only a limited faction (~70%) of total OC is water extractable (Chen and Bond, 2010). However, using methanol as extraction solvent, approximately up to 90% of total OC can be extracted (Chen and Bond, 2010; Cheng et al., 2017; Liu et al., 2013; Zhang et al., 2013). This study assesses the influence of fog-processing on light absorption properties of BrC. It is noteworthy that foggy events are prevalent during nighttime in the IGP. Thus, to differentiate the influence of fog on absorption properties of BrC, aerosol sampling was conducted during foggy and non-foggy episodes in nighttime. In this study, we report absorption properties of water extractable BrC (hereafter referred to as BrC) viz. absorption coefficient ($b_{abs\text{-}BrC\text{-}365}$), mass absorption efficiency ($MAE_{BrC\text{-}365}$), Absorption Ångström exponent (AAE) and absorbing component of refractive index ($k_{abs\text{-}BrC\text{-}365}$) from the central part of the IGP at Kanpur. Furthermore, absorption coefficient ($b_{abs\text{-}EC\text{-}660}$) and mass absorption efficiency ($MAE_{EC\text{-}660}$) of elemental carbon (EC) have also been assessed in this study. The observed absorption properties of both BrC and EC have been used to estimate the relative contribution of BrC in direct radiative forcing (DRF) in this study. Our results from the IGP on absorption properties and DRF of BrC and EC show contrasting features during foggy and non-foggy episodes.

2. Methodology

2.1. Site description

Sampling location (Kanpur: 26.30 °N, 80.14 °E, 142 m amsl) is situated in the central part of the IGP (Rajeev et al., 2016; Rajput et al., 2017). The IGP, stretch from NW to NE region in India, experiences severe fog and haze episodes during wintertime (December–February) (Rajput et al., 2015, 2016a). Fog episodes were quite frequent during the sampling period. Besides local sources, advective transport from upwind IGP influences atmospheric composition and chemistry over Kanpur (Rajput et al., 2016a, 2016b). The post-harvest agricultural-waste burning emission of paddy-residue (massive burning period: October–November) is an additional source of atmospheric carbonaceous aerosols during wintertime over the IGP (Rajput et al., 2014b).

2.2. Sampling procedure, meteorology and analysis

PM_1 (particulate matter with aerodynamic diameter ≤ 1 μm) samples have been collected during foggy nights (n = 17) and non-foggy nights (n = 19) onto pre-baked quartz fiber filters (Whatman™; 47 mm diameter) using a low-volume air-sampler (calibrated flow rate: 10 LPM) (Gupta et al., 2010; Kumar and Gupta, 2015) during November 2014–February 2015 continuously from 23:00 h to 7:00 h. More details about sampler characteristics are discussed in supplementary information. In this study, identification of foggy and non-foggy episodes has been made based on the meteorological informations retrieved from a nearby airport: Amausi (26.76 °N; 80.89 °E; 128 amsl) (Rajput et al., 2018). Ambient temperature, relative humidity (%) and visibility (km) during the study period are given in Table S2 of supplementary information. In this context, previous studies (UKMO, 1994; Vautard et al., 2009; WMO, 2005; Wu, 2006) have reported that foggy episodes are generally associated with low visibility (≤1 km) and high RH (≥90%) condition (Table S3).

PM_1 mass concentrations were measured gravimetrically post to equilibration of quartz filters at 25 ± 2 °C temperature and 40 ± 5% RH. For measurements of WSOC and absorbance signal due to water extractable BrC; a portion of each filter sample (3.14 cm^2) (pre-soaked overnight) was extracted (sonicated for 60 min = 30 + 20 + 10 min) thrice with 25 mL (total volume) of Milli-Q water (resistivity: 18.2 MΩ cm). As a matter of fact for sonication, bath sonication (power = 240 W) technique has been used. Soon after sonication, each extract was filtered through a 0.22 μm filter in amber colored glass vial. Subsequently, these samples were subjected for the determination of water-soluble organic carbon (WSOC) on a TOC analyzer (Shimadzu, LCPH). The absorbance signal due to BrC in each sample has been measured on a dual-channel UV-VIS spectrophotometer (Perkin Elmer; Model: Lambda 25), wherein baseline is monitored continuously with the solvent (Milli-Q) and corrected at each wavelength. Relevant informations on analytical determination of absorbance due to BrC on spectrophotometer are given in Table S1 and Fig. S1 (Supplementary Information). Concentration of K^+ in aerosols has been determined on an Ion-chromatograph (Metrohm) (Chakraborty and Gupta, 2010; Gupta and Mandaria, 2013; Rajput et al., 2016a). The measured K^+ concentrations, have been corrected for sea-salt and dust contributions to deduce its fraction from biomass burning emission (Keene et al., 1986; Rajput et al., 2014b). Mathematical equations to calculate biomass burning derived potassium (K^+_{BB}) have been discussed in supplementary information (Fig. S3). Similar to aerosol samples, blank filters (n = 4) were also processed and analyzed. Average blank values of WSOC, K^+ and OC corresponding to full-filter are 4.6 μg C, 3.4 μg and 3.4 μg C/cm^2, respectively, whereas that of absorbance is 0.16 at 365 nm. They constitute 2.5%, 19.8%, 6.2% and 9.3%, respectively of their average sample values. The reported concentrations of these parameters in aerosol samples have been corrected using average blank value. The concentrations of OC and EC (and its absorbance signal at 660 nm) have been measured by thermo-optical transmittance method using NIOSH (National Institute for Occupational Safety and Health) protocol on a Sunset Lab EC-OC analyzer (Birch and Cary, 1996; Rajput et al., 2017, 2018).

2.3. Absorption properties of brown carbon (BrC)

Absorption properties viz. absorption coefficient ($b_{abs\text{-}BrC\text{-}365}$), mass absorption efficiency ($MAE_{BrC\text{-}365}$), Absorption Ångström exponent (AAE) and absorbing component of refractive index ($k_{abs\text{-}BrC\text{-}365}$) have been assessed in this study. These properties of BrC have been assessed at 365 nm (Hecobian et al., 2010; Lukács et al., 2007). It is important to mention that absorbance at 365 nm is mainly due to BrC with some contributions from non-organic species such as nitrate, nitrite and metal-organic complexes etc. (Hecobian et al., 2010; Lukács et al., 2007). Accordingly, absorbance signal at 365 nm has been utilized for determination of $b_{abs\text{-}BrC\text{-}365}$ (1 Mm^{-1} = 10^{-6} m^{-1}) using following equation (Hecobian et al., 2010):

$$b_{abs-BrC-365}(Mm^{-1}) = \frac{[A_{365} \times V_l \times \ln(10) \times \text{Total filter area}]}{V_a \times L \times \text{filter area extracted}} \quad (1)$$

Here, A_{365} represents absorbance due to water-extractable BrC measured at 365 nm. V_l is volume of Milli-Q (m^3) utilized for extraction of aerosol sample, V_a refers to volume of air filtered (m^3) during aerosol sampling through filter-substrate and L indicates path-length of the cell (0.01 m). Total area of aerosol-laden filter is 13.85 cm^2, of which 3.14 cm^2 is extracted with Milli-Q and analyzed for determination of various parameters.

Due to current state of analytical limitations in resolving complex

Table 1
Absorption properties and direct radiative forcing of water-extractable BrC and EC associated with foggy and non-foggy events at Kanpur (in central IGP).

Parameters	Episode		*t*-test	Difference (p-value) (between non-foggy and foggy episodes)
	Non-foggy (n = 19)	Foggy (n = 17)		
PM_1 (μg/m^3)	263 ± 97	107 ± 58	5.8	***Significant (p < 0.05)***
WSOC (μg C/m^3)	28.8 ± 17.1	34.2 ± 17.8	0.9	Insignificant (p > 0.05)
EC (μg C/m^3)	8.6 ± 4.6	3.6 ± 3.0	3.8	***Significant (p < 0.05)***
WSOC/PM_1	0.11 ± 0.04	0.32 ± 0.05	14.0	***Significant (p < 0.05)***
EC/PM_1	0.03 ± 0.01	0.03 ± 0.01	0.9	Insignificant (p > 0.05)
WSOC/OC	0.42 ± 0.12	0.83 ± 0.10	11.1	***Significant (p < 0.05)***
OC/EC	8.4 ± 3.8	13.4 ± 3.8	3.9	***Significant (p < 0.05)***
$b_{abs\text{-}BrC\text{-}365}$ (Mm^{-1})	53.5 ± 19.5	69.3 ± 24.5	2.2	***Significant (p < 0.05)***
$MAE_{BrC\text{-}365}$ (m^2/g C)	1.6 ± 0.1	1.8 ± 0.2	3.8	***Significant (p < 0.05)***
$b_{abs\text{-}EC\text{-}660}$ (Mm^{-1})	56.1 ± 22.3	29.9 ± 19.6	3.7	***Significant (p < 0.05)***
$MAE_{EC\text{-}660}$ (m^2/g)	7.0 ± 0.5	8.5 ± 0.2	11.1	***Significant (p < 0.05)***
DRF_{BrC}/DRF_{EC} (%)	23.7 ± 10.8	54.3 ± 16.5	6.7	***Significant (p < 0.05)***

nature of myriads of compounds collectively termed as BrC, it is a widely followed practice to utilize WSOC concentration to represent the upper bound of water extractable BrC (Cheng et al., 2011; Choudhary et al., 2017; Hecobian et al., 2010; Laskin et al., 2015; Srinivas et al., 2016). MAE is expressed in m^2/g C and is determined using equation (2):

$$MAE_{BrC-365}(m^2/g\ C) = \frac{b_{abs-BrC-365}(Mm^{-1})}{WSOC(\mu g\ C/m^3)} \quad (2)$$

Hecobian et al. (2010) has suggested that properties of light absorbing aerosols exhibit a power law based spectral dependence as given below:

$$b_{abs-\lambda} = B\times \lambda^{-AAE} \quad (3)$$

In the above equation, B is a constant related to aerosol mass concentration, λ represents wavelength of light and AAE is Absorption Ångström exponent. The magnitude of AAE represents light absorption capacity of the concerned aerosol species. For example, Feng et al. (2013) has reported AAE ≈ 11 for moderately absorbing BrC and ≈ 6 for strongly absorbing BrC.

Basically, when light-beam passes through any medium, a fraction of light experiences attenuation in that medium. This attenuation can be represented mathematically by a complex term of refractive index ($m = k_{sca} \pm ik_{abs}$). Herein, k_{sca} and k_{abs} denote attenuation of light due to scattering and absorption by concerned species in the medium, respectively. The absorbing component of refractive index ($k_{abs\text{-}\lambda}$) can be estimated from equation (4) (Cheng et al., 2017; Shamjad et al., 2016):

$$k_{abs-\lambda} = \frac{\rho\times \lambda\times MAE_{\lambda}}{4\ \pi\times \left(\frac{OA}{OC}\right)} \quad (4)$$

Here, $k_{abs\text{-}\lambda}$ is a dimensionless entity and ρ is the density of BrC. Feng et al. (2013) has reported ρ of 1.65 g/cm^3 for BrC, whereas Hoffer et al. (2006) reported ρ of 1.57 g/cm^3. In this study, we have determined refractive index of BrC at 365 nm wavelength ($k_{abs\text{-}BrC\text{-}365}$) utilizing density of 1.65 g/cm^3. Moreover, OA/OC ratio of 1.7 has been used in this study (Rajput and Sarin, 2014).

2.4. Absorption properties of elemental carbon (EC)

In this study, absorption properties viz. absorption coefficient ($b_{abs\text{-}EC\text{-}660}$) and mass absorption efficiency (MAE_{660}) of EC at 660 nm were also assessed. Mathematical formulations to estimate absorption properties of EC are discussed as follows.

For the determination of $b_{abs\text{-}EC\text{-}660}$, following equation (Singh et al., 2014) has been considered:

$$b_{abs-EC-660} = \frac{A}{V}\times \frac{ATN}{R(ATN)\times C} \quad (5)$$

Here, $b_{abs\text{-}EC\text{-}660}$ is absorption coefficient of EC at 660 nm wavelength and expressed in Mm^{-1} (1M = 10^{-6}). ATN is attenuation signal of EC measured at 660 nm wavelength on EC-OC analyzer. "A" represents surface-area of aerosol laden filter. "V" denotes volume of air-filtered during each sample collection. C and R (ATN) are two empirical factors used to correct the measured attenuation signal due to multiple scattering and shadowing effect, respectively (Singh et al., 2014; Weingartner et al., 2003). In this study, R (ATN) and C value of 1 and 2.827 have been adopted from a previous study from IGP (Singh et al., 2014), respectively.

Mass absorption efficiency (MAE_{660}) of EC can be estimated from following relationship:

$$MAE_{EC-660}(m^2g^{-1}) = \frac{b_{abs-EC-660}}{EC(\mu g/m^3)} \quad (6)$$

3. Results and discussion

3.1. Mass concentration of WSOC and absorption coefficient of water extractable BrC ($b_{abs\text{-}BrC\text{-}365}$) over IGP

In this study, PM_1 mass concentration varied from 64 to 393 (Avg ± SD: 263 ± 97) μg/m^3 and 42–243 (107 ± 58) μg/m^3 during non-foggy and foggy nights, respectively. PM_1 mass concentrations have been discussed in Table S2 of supplementary information. A statistical description of absorption properties (b_{abs}, MAE) of BrC with chemical constituents of carbonaceous aerosols in PM_1 aerosols during foggy and non-foggy episodes are given in Table 1. As shown in Table 1, WSOC concentration varied from 6.8 to 65.6 (Avg ± SD: 28.2 ± 17.1 μg C/m^3) and 14.5–64.0 (34.2 ± 17.8 μg C/m^3) during non-foggy and foggy episodes, respectively. $b_{abs\text{-}BrC\text{-}365}$ varied from 27.4 to 91.8 (53.5 ± 19.5 Mm^{-1}) and 39.7–113.7 (69.3 ± 24.5 Mm^{-1}) during non-foggy and foggy episodes, respectively. Linear regression analysis (scatter plots) of $b_{abs\text{-}BrC\text{-}365}$ with K^+_{BB}, secondary organic carbon (SOC) and EC have been shown in Fig. 1a, b and c, respectively. Previous studies have suggested that biomass burning emission is a predominant source of organic carbon (OC: ~70%) in IGP, whereas fossil fuel combustion (60–90%) is dominant source of EC (Gustafsson et al., 2009; Rajput et al., 2014a; Venkataraman et al., 2005). In this context, a recent study (Vaishya et al., 2017) has also reported that dominant (~75%) fraction of EC in central IGP is derived from fossil fuel combustion. Thus, to decipher the predominant source of BrC, we have used K^+_{BB} as a tracer of biomass burning (Andreae, 1983; Rajput et al., 2014a) whereas EC was used for the fossil-fuel combustion source. Furthermore, to assess the origin of BrC from secondary sources, SOC has been estimated by OC/EC minimum ratio method (Castro

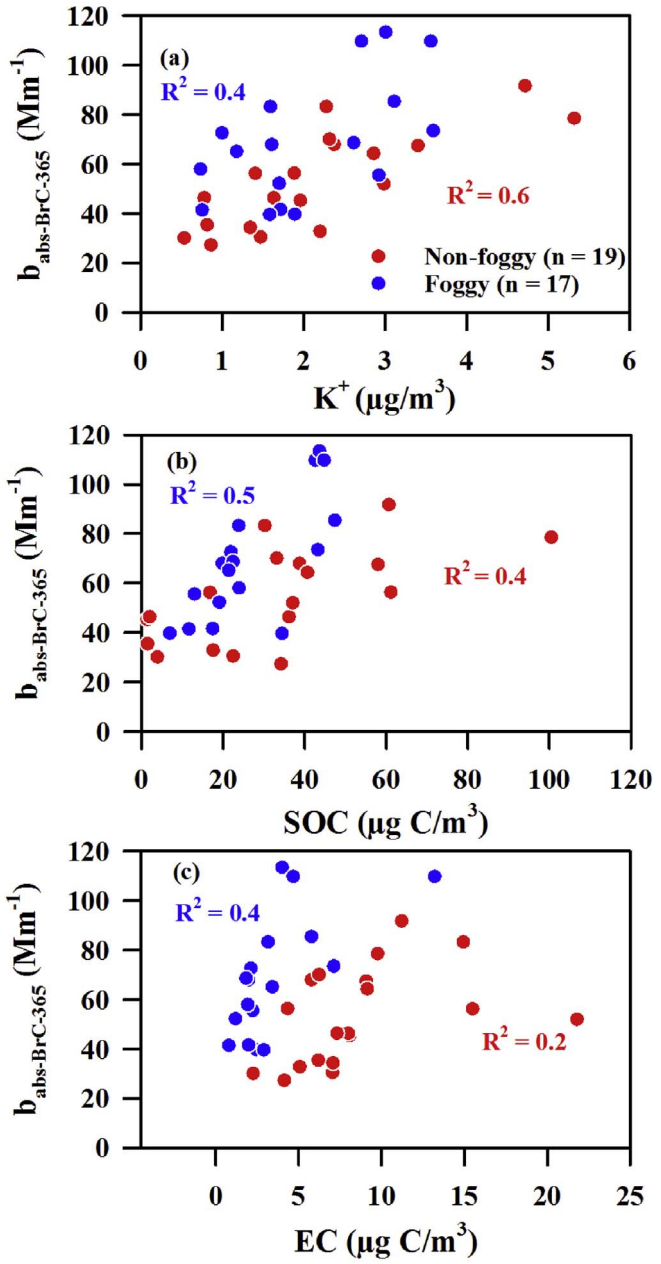

Fig. 1. Scatter plot of $b_{abs\text{-}BrC\text{-}365}$ with mass concentration of: (a) biomass burning derived potassium (K^{+}_{BB}) and (b) secondary organic carbon (SOC) and (c) EC in PM_1 during foggy and non-foggy episodes at Kanpur.

et al., 1999). The OC/EC minimum ratio method (Castro et al., 1999), is a near quantitative approach. It is worthwhile mentioning that due to less number of aerosol samples (n = 36), there might be inherent uncertainty on estimation of SOC. Previous studies have suggested that this method has uncertainty of ~20% in determining SOC (Na et al., 2004; Pio et al., 2011). Linear regression analyses of $b_{abs\text{-}BrC\text{-}365}$ with K^{+}_{BB} and SOC exhibit moderate correlation (Fig. 1a and b), whereas $b_{abs\text{-}BrC\text{-}365}$ with EC shows a weak correlation in this study. Thus, linear regression analysis suggests that biomass burning emission and secondary formations could be predominant sources of BrC over central IGP (Kanpur) during wintertime.

The WSOC mass concentration remained similar during non-foggy and foggy nights (non-foggy episode: 28.8 µg C/m^3; foggy episode: 34.2 µg C/m^3) (t-value = 0.9, difference is insignificant; Table 1). However, the average WSOC/PM_1 ratio during foggy nights was relatively high (0.32 ± 0.05) as compared to that during non-foggy nights (0.11 ± 0.04; Table 1). This is also reflected in higher WSOC/OC ratio during foggy episodes (0.83 ± 0.10) than the non-foggy episodes (0.42 ± 0.12). The elevated WSOC/PM_1, WSOC/OC and OC/EC ratio (Table 1) could be mainly due to fog-processing which leads to enhanced secondary organic aerosols (SOA) formation during foggy episodes (Kaul et al., 2011, 2012; Li et al., 2013). A strong correlation between SOC and WSOC mass concentration (R^2 = 0.9; Fig. S4) during foggy episodes reaffirmed the impact of fog processing on secondary formations. Influence of fog-processing was also observed on $b_{abs\text{-}BrC\text{-}365}$. Relatively high (t-value = 2.2, difference is significant) $b_{abs\text{-}BrC\text{-}365}$ (69.3 ± 24.5 Mm^{-1}) has been observed during foggy episodes as compared to that during non-foggy episodes (53.5 ± 19.5 Mm^{-1}). Several previous studies have suggested that fog-processing leads to oxidation of organic compounds (Chakraborty et al., 2016a, 2016b; Gilardoni et al., 2014). In this context, a recent study (Liu et al., 2015) has suggested that oxygenation of BrC might also lead to enhancement in their light absorption capacity. The $b_{abs\text{-}BrC\text{-}365}$ due to BrC during non-foggy episodes in this study at Kanpur (53.5 ± 19.5 Mm^{-1}) looks quite similar to that reported from an upwind IGP location at Patiala (52 ± 27 Mm^{-1}) (Srinivas et al., 2016). A significantly lower $b_{abs\text{-}BrC\text{-}365}$ of 11 ± 5 Mm^{-1} has been reported from a downwind location at Kharagpur (t = 13.9) (Srinivas and Sarin, 2014). Thus, a large variability in $b_{abs\text{-}BrC\text{-}365}$ is noteworthy from upwind to downwind locations in IGP. It should be noted that organic aerosol content can also be changed due to source variability.

3.2. Mass absorption efficiency (MAE) of BrC and EC over IGP

In this study, relatively low concentration (t = 3.8; p < 0.05; Table 1) of EC varying from 0.8 to 13.2 (3.6 ± 3.0) µg C/m^3 has been observed during foggy episodes as compared to that during non-foggy episodes [range: 2.3–21.8; Avg. ± SD: 8.6 ± 4.6 µg/m^3]. It is important to mention here that unlike absorption coefficient of BrC, $b_{abs\text{-}EC\text{-}660}$ during foggy episodes [range: 8.5–88.4 (29.9 ± 19.6) Mm^{-1}] is relatively low compared to the non-foggy episodes [range: 17.6–108.2 (56.1 ± 22.3) Mm^{-1}]. The lower value of $b_{abs\text{-}EC\text{-}660}$ during foggy events is attributable to lower abundance of EC. The $b_{abs\text{-}EC\text{-}660}$ and EC concentration exhibits a strong linear relationship shown in Fig. 2a, indicating validity of Beer-Lambert's law. However, this linearity does not extend beyond data-points with EC concentration > 12 µg C/m^3 shown in Fig. 2a (separated by vertical dashed line), and thus data points with higher values of EC > 12 µg C/m^3 were not considered for regression analysis in Fig. 2a. The slope of linear regression analysis in Fig. 2a represents $MAE_{EC\text{-}660}$. The $MAE_{EC\text{-}660}$ during foggy episodes [range: 6.7–10.6 (8.5 ± 0.2) m^2/g] is relatively high (t = 11.1; p < 0.05; Table 1) as compared to 5.0–7.8 (7.0 ± 0.5) m^2/g during non-foggy episodes (Fig. 2a). The enhancement in $MAE_{EC\text{-}660}$ (by ~ 20%) during foggy events could be attributed to source variability and/or change in morphology/mixing state and lensing effect due to coating on EC (core) surface through fog-processing. However, similar EC/PM_1 ratio (Table 1) during foggy and non-foggy episodes indicates that sources of EC remained more or less similar during foggy and non-foggy episodes. Thus, enhancement in MAE of EC due to fog-processing can mainly be attributable to change in mixing state/morphology and lensing effect (due to coating on EC) (Schmid et al., 2006; Schwarz et al., 2008).

Linear regression analysis between $b_{abs\text{-}BrC\text{-}365}$ and WSOC is shown in Fig. 2b. Slope of linear regression for these two parameters represents $MAE_{BrC\text{-}365}$. Similar to EC, $MAE_{BrC\text{-}365}$ during foggy episodes [range: 1.2–3.1 (1.8 ± 0.2) m^2/g C] is relatively high (t = 3.8; p < 0.05; Table 1) as compared to that during non-foggy episodes [range: 1.1–4.1 (1.6 ± 0.1) m^2/g C]. Enhancement in $MAE_{BrC\text{-}365}$ (by ~ 15%) during foggy events was consistent with that observed in WSOC/OC, WSOC/PM_1, OC/EC and $b_{abs\text{-}BrC\text{-}365}$. Uncertainty on MAE of BrC is about ± 7% [deduced from replicate measurements (n = 10) of aerosol aqueous extracts].

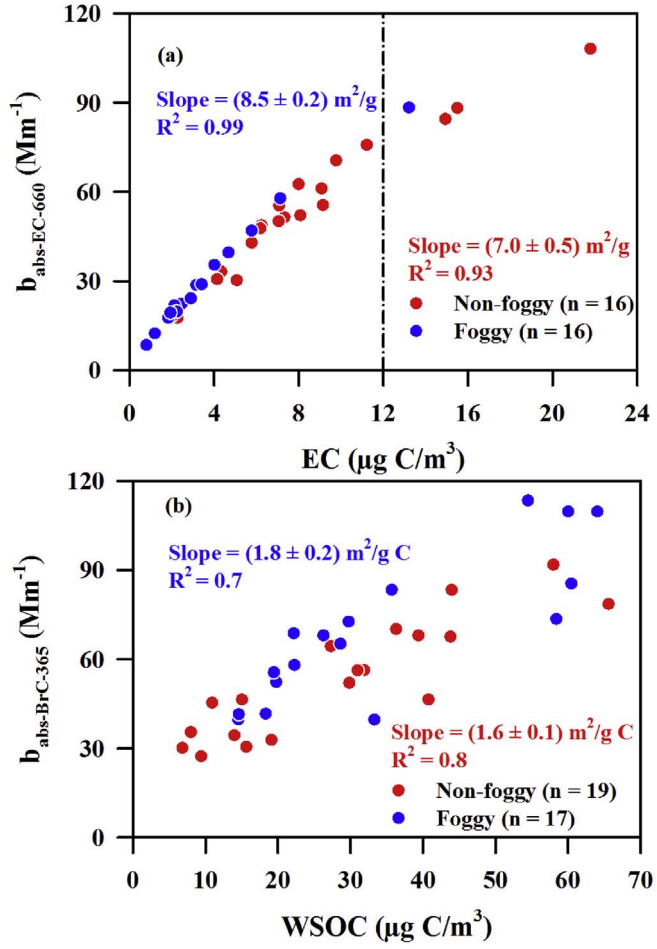

Fig. 2. Scatter plot of absorption coefficient of: (a) EC ($b_{abs\text{-}EC\text{-}660}$) with its mass concentration and (b) water-extractable BrC ($b_{abs\text{-}BrC\text{-}365}$) with WSOC in PM_1 during foggy and non-foggy episodes at Kanpur. Data-points with EC concentration > 12 µg C/m^3 (separated by vertical dashed line) have not been considered for regression analysis in Fig. 2a.

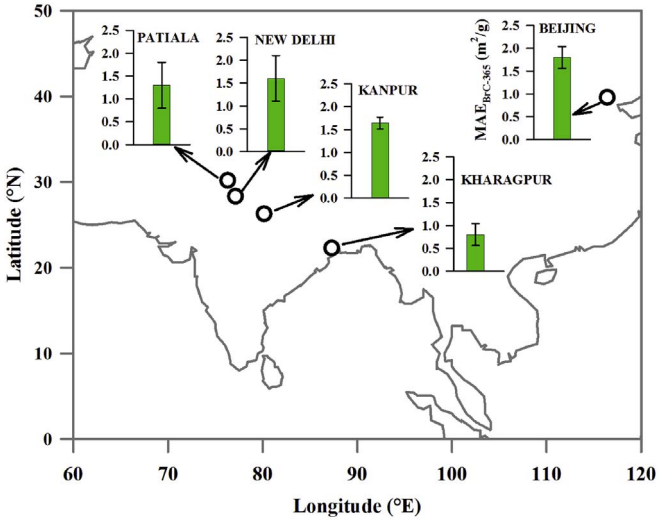

Fig. 3. Mass absorption efficiency of water-extractable brown carbon ($MAE_{BrC\text{-}365}$) from different study locations in Indo-Gangetic Plain: Kanpur (this study, non-foggy; n = 19), Patiala (Srinivas et al., 2016), Delhi (Kirillova et al., 2014), and Kharagpur (Srinivas and Sarin, 2014). For the sake of comparison, we have also shown data set of $MAE_{BrC\text{-}365}$ from Beijing (Cheng et al., 2011). Here, error-bars represent variability of $MAE_{BrC\text{-}365}$ during the study period.

In Fig. 3, $MAE_{BrC\text{-}365}$ (water-extractable fraction) at Kanpur has been compared with those reported in different studies. In this study (at Kanpur), the $MAE_{BrC\text{-}365}$ averages at 1.6 ± 0.1 m^2/g C (non-foggy events). Previous studies from upwind (Patiala) and downwind IGP locations (Kharagpur) have reported $MAE_{BrC\text{-}365}$ of: 1.3 ± 0.5 and 0.8 ± 0.2 m^2/g C, respectively (Srinivas et al., 2016; Srinivas and Sarin, 2014). A study at New Delhi (Kirillova et al., 2014) (another location in upwind IGP) reported $MAE_{BrC\text{-}365}$ of 1.6 ± 0.5 m^2/g C (Fig. 3). In their study, they have concluded that at New Delhi, ~80% of WSOC is derived from biomass burning emission whereas fossil-fuel combustion contributed to a smaller fraction (20%). Another study from Beijing has also reported $MAE_{BrC\text{-}365}$ of 1.8 ± 0.2 m^2/g C from biomass burning emission (Cheng et al., 2011). Summing up, $MAE_{BrC\text{-}365}$ (water-extractable: 1.6 m^2/g C) observed at Kanpur is near similar to that reported for predominant biomass burning emission at Patiala, New Delhi and Beijing discussed herein.

3.3. Absorption Ångström exponent (AAE) and absorbing component of refractive index (k_{abs}) of BrC

Light absorbing aerosols generally exhibit a spectral dependence following the power law (as shown in equation (3)). For the estimation of AAE of BrC, first we have calculated $b_{abs\text{-}\lambda}$ at 16 wavelengths (300, 325, 350, 365, 375, 400, 425, 450, 475, 500, 550, 600, 625, 650, 675 and 700 nm). Subsequently, by using power-fit, the spectral dependence of $b_{abs\text{-}\lambda}$ has been assessed as a function of wavelength (λ) (Fig. 4a). Different spectral lines in the plot represent b_{abs} in different aerosol aqueous extracts. The power fit in the plot gives AAE value of BrC (at Kanpur; this study); varying from 1.7 to 3.9 (2.8 ± 0.6) in this study. Furthermore, spread (= 0.6) on average value of AAE over the sampling period is given on Fig. 4a. Based on replicate measurements (n = 10), analytical uncertainty on AAE has been determined to be within ± 7.0%. In this study, AAE during non-foggy (1.7–3.9) and foggy (2.0–3.6) episodes look nearly identical. This observation suggests that sources contribution and/or their combustion condition during the entire sampling period is more or the less uniform. Previous studies have reported AAE value of 5.3 ± 2.0, 5.1 ± 2.0 and 6.0 ± 1.1 in $PM_{2.5}$ bound BrC aerosols from Patiala, New Delhi and Kharagpur in IGP, respectively (Kirillova et al., 2014; Srinivas et al., 2016; Srinivas and Sarin, 2014). Furthermore, AAE value ($PM_{2.5}$ bound) of 7.2 ± 0.3 and 7.6 ± 0.5 have been documented at Beijing (Cheng et al., 2017) and Los Angeles (Zhang et al., 2013), respectively. In this context, it is noteworthy that this study reports AAE (a size dependent parameter) of PM_1 bound BrC aerosols. Moreover, previous studies (Chen and Bond, 2010; Lu et al., 2015; Saleh et al., 2014) have reported that difference in biomass types and combustion condition could also lead to significant variability in AAE of BrC. In the same context, a previous study (Feng et al., 2013) has reported AAE value of ~11 due to moderately absorbing BrC, whereas AAE value of 6.6 (or even lower) is due to strongly absorbing BrC. Similar observations have been reported by another study (Chung et al., 2012), suggesting that strongly absorbing BrC exhibits higher MAE and lower AAE value. Thus, significantly lower values of AAE (in this study) compared to other places in IGP highlights more light absorbing potential of atmospheric BrC over central IGP.

It is very important to mention here that $k_{abs\text{-}\lambda}$ of BrC and its spectral dependence has been reported by very few studies. Using equation (4), we have calculated $k_{abs\text{-}\lambda}$ at 16 wavelengths (300, 325, 350, 365, 375, 400, 425, 450, 475, 500, 550, 600, 625, 650, 675 and 700 nm). Throughout this study, $k_{abs\text{-}BrC\text{-}365}$ varied from 0.03 to 0.13 (0.07 ± 0.03). A study from biomass burning emissions viz. savanna forest-fires (southern Africa) (Kirchstetter et al., 2004) has reported higher $k_{abs\text{-}BrC\text{-}350}$ of 0.2. Another study from wood-combustion source has reported a value of 0.1 for $k_{abs\text{-}BrC\text{-}350}$ (Chen and Bond, 2010). Thus, based on previous studies, it can be summarized that there is a large variability in refractive index of BrC for different types of biomass

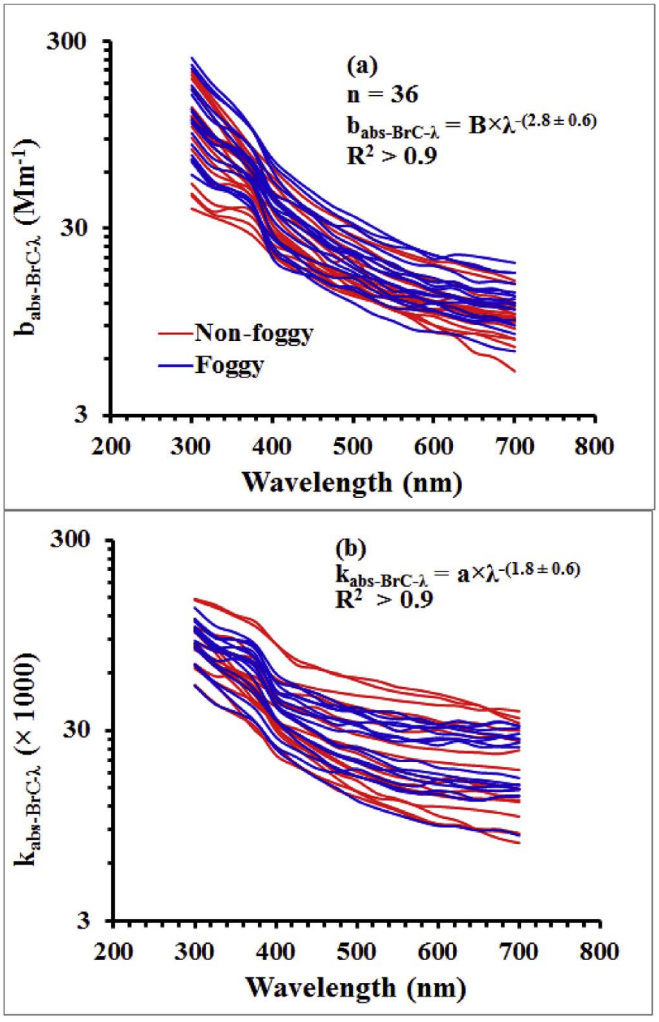

Fig. 4. Plots showing spectral dependence of: (a) absorption coefficient ($b_{abs\text{-}\lambda}$) and (b) absorbing component of refractive index ($k_{abs\text{-}\lambda}$) of BrC during non-foggy and foggy episodes in this study.

burning emissions (agricultural residue, wood-burning and forest-fires). By using power fit, the spectral dependence of $k_{abs\text{-}\lambda}$ has been assessed for the aerosol aqueous extracts and represented in Fig. 4b. Interestingly, we observe a significant difference in spectral behavior of $b_{abs\text{-}\lambda}$ and $k_{abs\text{-}\lambda}$ (Fig. 4a and b). The most plausible reason for this observation is attributable to significant difference in the magnitude (2.8 versus 1.8) of their spectral dependence: $b_{abs\text{-}\lambda}$ α $\lambda^{-(2.8 \pm 0.6)}$ and $k_{abs\text{-}\lambda}$ α $\lambda^{-(1.8 \pm 0.6)}$.

3.4. Direct radiative forcing of BrC (relative to that of EC)

Light absorbing aerosol species contribute to the total perturbation in earth's radiation budget. This phenomenon results in a significant change in average temperature (per decade) of the earth's atmosphere (Ramanathan et al., 2007). Thus, the determination of DRF due to BrC has significance in general and particularly over tropical region owing to massive loading of organic aerosols (Andreae and Merlet, 2001; Rajput et al., 2014b). Towards this, we have first determined light attenuation due to absorption by BrC and EC using an approach suggested by previous studies (Kirillova et al., 2014; Srinivas et al., 2016; Srinivas and Sarin, 2014). Accordingly, the light attenuation due to absorption by BrC and EC can be quantitatively represented by Beer-Lambert's law as follows:

$$\frac{I_o - I}{I_o}(\lambda, \text{BrC}) = 1 - e^{-\left(\text{MAE}_{365} \times \left(\frac{\lambda_o}{\lambda}\right)^{\text{AAE}} \times C_{\text{WSOC}} \times h_{\text{ABL}}\right)} \quad (7)$$

$$\frac{I_o - I}{I_o}(\lambda, \text{EC}) = 1 - e^{-\left(\text{MAE}_{660} \times \left(\frac{\lambda_o}{\lambda}\right)^{\text{AAE}} \times C_{\text{EC}} \times h_{\text{ABL}}\right)} \quad (8)$$

Here, MAE_{365} and MAE_{660} represent MAE of BrC and EC at a reference wavelength (λ_o); λ_o at 365 and 660 nm are widely used for BrC and EC, respectively. λ refers to any wavelength between 300 and 2500 nm. C_{wsoc} and C_{EC} represent mass concentration (g C/m^3) of water-soluble organic carbon (WSOC) and elemental carbon (EC) respectively. h_{ABL} refers to atmospheric boundary layer height in meters. During winter season, the h_{ABL} averages at around 1000 m over IGP.

Subsequently, the DRF of BrC relative to that of EC (DRF_{BrC}/DRF_{EC}) across the solar spectrum (300–2500 nm) has been estimated by multiplying solar emission flux with light absorption attenuation due to BrC and normalized with that of EC (Kirillova et al., 2014; Srinivas et al., 2016). The contribution of DRF of BrC relative to that of EC can be mathematically expressed as follows:

$$f = \frac{\int_{300}^{2500} I_o(\lambda)\left[\frac{I_o - I}{I_o}(\lambda, \text{BrC})\right] d\lambda}{\int_{300}^{2500} I_o(\lambda)\left[\frac{I_o - I}{I_o}(\lambda, \text{EC})\right] d\lambda} \quad (9)$$

Here, $I_o(\lambda)$ represents the solar emission flux or spectral irradiance (W/m^2/nm) during clear sky condition. $I_o(\lambda)$ values have been retrieved from Air Mass 1 Global Horizontal (AM1GH) solar irradiance model (Levinson et al., 2010).

In this study, AAE (= 1) of EC has been adopted from previous studies (Bond and Bergstrom, 2006; Cheng et al., 2011; Kirchstetter and Thatcher, 2012; Kirillova et al., 2014). Using equations (7)–(9), atmospheric DRF of BrC relative to that of EC has been estimated from numerical analysis technique (Simpson's 1/3rd rule) with data input at 50 nm interval. Atmospheric DRF of BrC (relative to that of EC; Fig. 5),

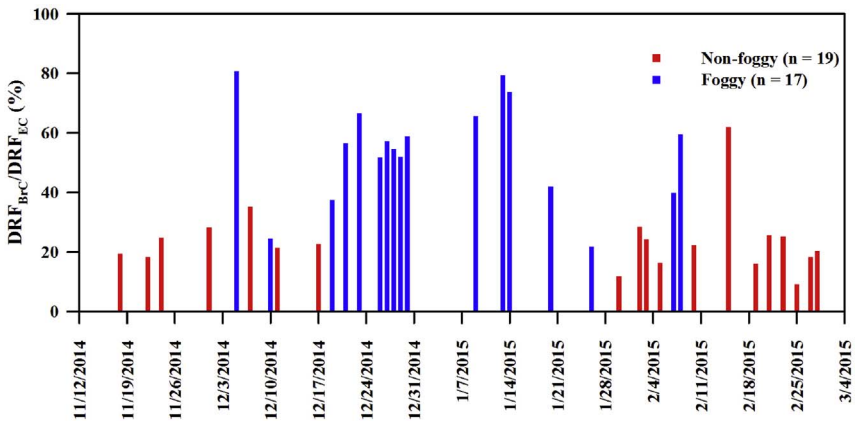

Fig. 5. Atmospheric direct radiative forcing of BrC (relative to EC) in PM_1 during non-foggy and foggy episodes at Kanpur in Indo-Gangetic Plain.

centers at 23.7 ± 10.8 (9.2–61.9) % during non-foggy days whereas, during foggy episodes it averages at relatively high value (by a factor of 2) of 54.3 ± 16.5 (21.8–80.2) %. It is important to mention here that absorption properties and DRF of BrC reported herein during the foggy episodes represents their values due to collected submicron (≤1 μm) fog drops and particulate matter. The large difference in DRF of BrC (relative to EC) during foggy episodes as compared to that during non-foggy episodes has also been affirmed based on statistical two-tailed *t*-test ($p < 0.05$; Table 1). Previous studies (Srinivas et al., 2016; Srinivas and Sarin, 2014), have also reported that atmospheric DRF of BrC (relative to that of EC) centered at ~ 40% over upwind IGP (Patiala) and ~17% at downwind IGP (Kharagpur). Thus, our study in conjunction with previous studies suggests that BrC represents a significant contribution to atmospheric radiative forcing due to aerosols during wintertime over the IGP.

4. Conclusions

PM_1 samples were collected on foggy and non-foggy nights (during wintertime) from Kanpur location in central part of Indo-Gangetic Plain. Characteristic absorption properties of BrC and EC have been studied to understand the impact of fog-processing. Important outcomes of this study are summarized below:

(1) Biomass burning emission and secondary transformations of VOCs appeared to be predominant sources of BrC during wintertime over central IGP.
(2) MAE of BrC and EC exhibit enhancement by ~ 15% and ~ 20%, respectively during foggy episodes.
(3) Significantly lower value of AAE (2.8) compared to other places in IGP (~5) highlights more light absorbing potential of atmospheric BrC over central IGP.
(4) DRF of BrC (relative to that of EC) during foggy episodes is relatively high (by a factor of 2) as compared to that during non-foggy episodes. This has been attributed mainly to influence of fog-processing. Furthermore, we urge that future modeling studies can consider the herein reported enhancement factor for estimating DRF during foggy episodes over IGP.

Acknowledgements

This study has been carried out with aid of internal funds from IIT Kanpur and partial funds were provided by Indian National Science Academy (INSA Grant # SP/YSP/113/2015(1091)) to Tarun Gupta to complete this study. The Authors acknowledge anonymous reviewers for their constructive comments and suggestions and Dr. Mustafa Odabasi for editorial handling of this manuscript. PR is thankful to Council of Scientific & Industrial Research for providing CSIR-Senior Research Associate fellowship (Pool No: 8934-A/2017).

Appendix A. Supplementary data

Supplementary data related to this article can be found at http://dx.doi.org/10.1016/j.apr.2017.11.012.

References

Andreae, M.O., 1983. Soot carbon and excess fine potassium: long-range transport of combustion-derived aerosols. Science 220, 1148–1151.
Andreae, M.O., Gelencser, A., 2006. Black carbon or brown carbon? The nature of light-absorbing carbonaceous aerosols. Atmos. Chem. Phys. 6, 3419–3463.
Andreae, M.O., Merlet, P., 2001. Emission of trace gases and aerosols from biomass burning. Global Biogeochem. Cycles 15, 955–966.
Artaxo, P., Martins, J.V., Yamasoe, M.A., Procópio, A.S., Pauliquevis, T.M., Andreae, M.O., Guyon, P., Gatti, L.V., Leal, A.M.C., 2002. Physical and chemical properties of aerosols in the wet and dry seasons in Rondônia, Amazonia. J. Geophys. Res. Atmos. 107 LBA 49-41-LBA 49–14.
Birch, M.E., Cary, R.A., 1996. Elemental carbon-based method for monitoring occupational exposures to particulate diesel exhaust. Aerosol. Sci. Technol. 25, 221–241.
Bond, T.C., Bergstrom, R.W., 2006. Light absorption by carbonaceous particles: an investigative review. Aerosol. Sci. Technol. 40, 27–67.
Castro, L.M., Pio, C.A., Harrison, R.M., Smith, D.J.T., 1999. Carbonaceous aerosol in urban and rural European atmospheres: estimation of secondary organic carbon concentrations. Atmos. Environ. 33, 2771–2781.
Chakraborty, A., Ervens, B., Gupta, T., Tripathi, S.N., 2016a. Characterization of organic residues of size-resolved fog droplets and their atmospheric implications. J. Geophys. Res.: Atmos. 121, 4317–4332.
Chakraborty, A., Gupta, T., 2010. Chemical characterization and source apportionment of submicron (PM_1) aerosol in kanpur region. Aerosol Air Qual. Res. 10, 433–445.
Chakraborty, A., Gupta, T., Tripathi, S.N., 2016b. Combined effects of organic aerosol loading and fog processing on organic aerosols oxidation, composition, and evolution. Sci. Total Environ. 573, 690–698.
Chakraborty, A., Rajeev, P., Rajput, P., Gupta, T., 2017. Water soluble organic aerosols in indo gangetic plain (IGP): insights from aerosol mass spectrometry. Sci. Total Environ. 599, 1573–1582.
Chen, Y., Bond, T.C., 2010. Light absorption by organic carbon from wood combustion. Atmos. Chem. Phys. 10, 1773–1787.
Cheng, Y., He, K.-b., Du, Z.-y., Engling, G., Liu, J.-m., Ma, Y.-l., Zheng, M., Weber, R.J., 2016. The characteristics of brown carbon aerosol during winter in Beijing. Atmos. Environ. 127, 355–364.
Cheng, Y., He, K.-b., Engling, G., Weber, R., Liu, J.-m., Du, Z.-y., Dong, S.-p., 2017. Brown and black carbon in Beijing aerosol: implications for the effects of brown coating on light absorption by black carbon. Sci. Total Environ. 599–600, 1047–1055.
Cheng, Y., He, K.B., Zheng, M., Duan, F.K., Du, Z.Y., Ma, Y.L., Tan, J.H., Yang, F.M., Liu, J.M., Zhang, X.L., Weber, R.J., Bergin, M.H., Russell, A.G., 2011. Mass absorption efficiency of elemental carbon and water-soluble organic carbon in Beijing, China. Atmos. Chem. Phys. 11, 11497–11510.
Choudhary, V., Rajput, P., Rajeev, P., Gupta, T., 2017. Synergistic effect in absorption properties of brown carbon and elemental carbon over IGP during weak south-west monsoon. Aerosol Sci. Eng. 1 (3), 138–149.
Chung, C.E., Ramanathan, V., Decremer, D., 2012. Observationally constrained estimates of carbonaceous aerosol radiative forcing. Proc. Natl. Acad. Sci. U. S. A. 109, 11624–11629.
Feng, Y., Ramanathan, V., Kotamarthi, V.R., 2013. Brown carbon: a significant atmospheric absorber of solar radiation? Atmos. Chem. Phys. 13, 8607–8621.
Gilardoni, S., Massoli, P., Giulianelli, L., Rinaldi, M., Paglione, M., Pollini, F., Lanconelli, C., Poluzzi, V., Carbone, S., Hillamo, R., Russell, L.M., Facchini, M.C., Fuzzi, S., 2014. Fog scavenging of organic and inorganic aerosol in the Po Valley. Atmos. Chem. Phys. 14, 6967–6981.
Gupta, T., Chakraborty, A., Ujinwal, K.K., 2010. Development and performance evaluation of an indigenously developed air sampler designed to collect submicron aerosol. Ann. Indian Natl. Acad. Eng. (INAE) 7, 189–193.
Gupta, T., Mandaria, A., 2013. Sources of submicron aerosol during fog dominated wintertime at Kanpur. Environ. Sci. Pollut. Res. http://dx.doi.org/10.1007/s11356-11013-11580-11356.
Gustafsson, Ö., Kruså, M., Zencak, Z., Sheesley, R.J., Granat, L., Engström, E., Praveen, P.S., Rao, P.S.P., Leck, C., Rodhe, H., 2009. Brown Clouds over South Asia: biomass or fossil fuel combustion? Science 323, 495–498.
Hecobian, A., Zhang, X., Zheng, M., Frank, N., Edgerton, E.S., Weber, R.J., 2010. Water-Soluble Organic Aerosol material and the light-absorption characteristics of aqueous extracts measured over the Southeastern United States. Atmos. Chem. Phys. 10, 5965–5977.
Hoffer, A., Gelencsér, A., Guyon, P., Kiss, G., Schmid, O., Frank, G.P., Artaxo, P., Andreae, M.O., 2006. Optical properties of humic-like substances (HULIS) in biomass-burning aerosols. Atmos. Chem. Phys. 6, 3563–3570.
Hoffer, A., Kiss, G., Blazsó, M., Gelencsér, A., 2004. Chemical characterization of humic-like substances (HULIS) formed from a lignin-type precursor in model cloud water. Geophys. Res. Lett. 31. http://dx.doi.org/10.1029/2003GL018962.
Kaul, D.S., Gupta, T., Tripathi, S.N., 2012. Chemical and microphysical properties of the aerosol during foggy and nonfoggy episodes: a relationship between organic and inorganic content of the aerosol. Atmos. Chem. Phys. Discuss. 2012, 14483–14524.
Kaul, D.S., Gupta, T., Tripathi, S.N., Tare, V., Collett, J.L., 2011. Secondary organic aerosol: a comparison between foggy and nonfoggy days. Environ. Sci. Technol. 45, 7307–7313.
Keene, W.C., Pszenny, A.A.P., Galloway, J.N., Hawley, M.E., 1986. Sea-salt corrections and interpretation of constituent ratios in marine precipitation. J. Geophys. Res.: Atmos. 91, 6647–6658.
Kirchstetter, T.W., Novakov, T., Hobbs, P.V., 2004. Evidence that the spectral dependence of light absorption by aerosols is affected by organic carbon. J. Geophys. Res.: Atmos. 109, D21208.
Kirchstetter, T.W., Thatcher, T.L., 2012. Contribution of organic carbon to wood smoke particulate matter absorption of solar radiation. Atmos. Chem. Phys. 12, 6067–6072.
Kirillova, E.N., Andersson, A., Tiwari, S., Srivastava, A.K., Bisht, D.S., Gustafsson, Ö., 2014. Water-soluble organic carbon aerosols during a full New Delhi winter: isotope-based source apportionment and optical properties. J. Geophys. Res.: Atmos. 119, 3476–3485.
Kumar, A., Gupta, T., 2015. Development and field evaluation of a multiple slit nozzle-based high volume $PM_{2.5}$ inertial impactor assembly (hvia). Aerosol Air Qual. Res. 15, 1188–1200.
Kumar, V., Goel, A., Rajput, P., 2017. Compositional and surface characterization of HULIS by UV-Vis, FTIR, NMR and XPS: wintertime study in Northern India. Atmos. Environ. 164, 468–475.
Lack, D.A., Bahreini, R., Langridge, J.M., Gilman, J.B., Middlebrook, A.M., 2013. Brown

carbon absorption linked to organic mass tracers in biomass burning particles. Atmos. Chem. Phys. 13, 2415–2422.
Laskin, A., Laskin, J., Nizkorodov, S.A., 2015. Chemistry of atmospheric brown carbon. Chem. Rev. 115, 4335–4382.
Lee, H.J., Aiona, P.K., Laskin, A., Laskin, J., Nizkorodov, S.A., 2014. Effect of solar radiation on the optical properties and molecular composition of laboratory proxies of atmospheric brown carbon. Environ. Sci. Technol. 48, 10217–10226.
Levinson, R., Akbari, H., Berdahl, P., 2010. Measuring solar reflectance—Part I: defining a metric that accurately predicts solar heat gain. Sol. Energy 84, 1717–1744.
Li, Y.J., Lee, B.Y.L., Yu, J.Z., Ng, N.L., Chan, C.K., 2013. Evaluating the degree of oxygenation of organic aerosol during foggy and hazy days in Hong Kong using high-resolution time-of-flight aerosol mass spectrometry (HR-ToF-AMS). Atmos. Chem. Phys. 13, 8739–8753.
Liu, J., Bergin, M., Guo, H., King, L., Kotra, N., Edgerton, E., Weber, R.J., 2013. Size-resolved measurements of brown carbon in water and methanol extracts and estimates of their contribution to ambient fine-particle light absorption. Atmos. Chem. Phys. 13, 12389–12404.
Liu, S., Aiken, A.C., Gorkowski, K., Dubey, M.K., Cappa, C.D., Williams, L.R., Herndon, S.C., Massoli, P., Fortner, E.C., Chhabra, P.S., Brooks, W.A., Onasch, T.B., Jayne, J.T., Worsnop, D.R., China, S., Sharma, N., Mazzoleni, C., Xu, L., Ng, N.L., Liu, D., Allan, J.D., Lee, J.D., Fleming, Z.L., Mohr, C., Zotter, P., Szidat, S., Prévôt, A.S.H., 2015. Enhanced light absorption by mixed source black and brown carbon particles in UK winter. Nat. Commun. 6, 8435.
Lu, Z., Streets, D.G., Winijkul, E., Yan, F., Chen, Y., Bond, T.C., Feng, Y., Dubey, M.K., Liu, S., Pinto, J.P., Carmichael, G.R., 2015. Light absorption properties and radiative effects of primary organic aerosol emissions. Environ. Sci. Technol. 49, 4868–4877.
Lukács, H., Gelencsér, A., Hammer, S., Puxbaum, H., Pio, C., Legrand, M., Kasper-Giebl, A., Handler, M., Limbeck, A., Simpson, D., Preunkert, S., 2007. Seasonal trends and possible sources of brown carbon based on 2-year aerosol measurements at six sites in Europe. J. Geophys. Res. Atmos. 112. http://dx.doi.org/10.1029/2006JD008151.
Massabò, D., Caponi, L., Bove, M.C., Prati, P., 2016. Brown carbon and thermal–optical analysis: a correction based on optical multi-wavelength apportionment of atmospheric aerosols. Atmos. Environ. 125, 119–125.
Na, K., Sawant, A.A., Song, C., Cocker III, D.R., 2004. Primary and secondary carbonaceous species in the atmosphere of Western Riverside County, California. Atmos. Environ. 38, 1345–1355.
Park, R.J., Kim, M.J., Jeong, J.I., Youn, D., Kim, S., 2010. A contribution of brown carbon aerosol to the aerosol light absorption and its radiative forcing in East Asia. Atmos. Environ. 44, 1414–1421.
Pavuluri, C.M., Kawamura, K., Swaminathan, T., Tachibana, E., 2011. Stable carbon isotopic compositions of total carbon, dicarboxylic acids and glyoxylic acid in the tropical Indian aerosols: implications for sources and photochemical processing of organic aerosols. J. Geophys. Res. Atmos. 116, D18307.
Pio, C., Cerqueira, M., Harrison, R.M., Nunes, T., Mirante, F., Alves, C., Oliveira, C., Sanchez de la Campa, A., Artíñano, B., Matos, M., 2011. OC/EC ratio observations in Europe: Re-thinking the approach for apportionment between primary and secondary organic carbon. Atmos. Environ. 45, 6121–6132.
Rajeev, P., Rajput, P., Gupta, T., 2016. Chemical characteristics of aerosol and rain water during an El Niño and PDO influenced Indian summer monsoon. Atmos. Environ. 145, 192–200.
Rajput, P., Anjum, M.H., Gupta, T., 2017. One year record of bioaerosols and particles concentration in Indo-Gangetic Plain: implications of biomass burning emissions to high-level of endotoxin exposure. Environ. Pollut. 224, 98–106.
Rajput, P., Gupta, T., Kumar, A., 2016a. The diurnal variability of sulfate and nitrate aerosols during wintertime in the Indo-Gangetic Plain: implications for heterogeneous phase chemistry. RSC Adv. 6, 89879–89887.
Rajput, P., Mandaria, A., Kachawa, L., Singh, D.K., Singh, A.K., Gupta, T., 2015. Wintertime source-apportionment of PM_1 from Kanpur in the Indo-Gangetic Plain. Climate Change 1, 503–507.
Rajput, P., Mandaria, A., Kachawa, L., Singh, D.K., Singh, A.K., Gupta, T., 2016b. Chemical characterisation and source apportionment of PM_1 during massive loading at an urban location in Indo-Gangetic Plain: impact of local sources and long-range transport. Tellus B 68, 30659.
Rajput, P., Sarin, M.M., 2014. Polar and non-polar organic aerosols from large-scale agricultural-waste burning emissions in Northern India: implications to organic mass-to-organic carbon ratio. Chemosphere 103, 74–79.
Rajput, P., Sarin, M.M., Sharma, D., Singh, D., 2014a. Characteristics and emission budget of carbonaceous species from post-harvest agricultural-waste burning in source region of the Indo-Gangetic Plain. Tellus B. http://dx.doi.org/10.3402/tellusb.v66.21026.
Rajput, P., Sarin, M.M., Sharma, D., Singh, D., 2014b. Organic aerosols and inorganic species from post-harvest agricultural-waste burning emissions over northern India: impact on mass absorption efficiency of elemental carbon. Environ. Sci.: Process. Impacts 16, 2371–2379.
Rajput, P., Singh, D.K., Singh, A.K., Gupta, T., 2018. Chemical composition and source-apportionment of sub-micron particles during wintertime over Northern India: New insights on influence of fog-processing. Environ. Pollut. 233, 81–91.
Ram, K., Sarin, M.M., 2009. Absorption coefficient and site-specific mass absorption efficiency of elemental carbon in aerosols over urban, rural, and high-altitude sites in India. Environ. Sci. Technol. 43, 8233–8239.
Ram, K., Sarin, M.M., Sudheer, A.K., Rengarajan, R., 2012. Carbonaceous and secondary inorganic aerosols during wintertime fog and haze over urban sites in the Indo-Gangetic Plain. Aerosol Air Qual. Res. 12, 359–370.
Ramanathan, V., Carmichael, G., 2008. Global and regional climate changes due to black carbon. Nat. Geosci. 1, 221.
Ramanathan, V., Ramana, M.V., Roberts, G., Kim, D., Corrigan, C., Chung, C., Winker, D., 2007. Warming trends in Asia amplified by brown cloud solar absorption. Nature 448, 575–578.
Rengarajan, R., Sarin, M.M., Sudheer, A.K., 2007. Carbonaceous and inorganic species in atmospheric aerosols during wintertime over urban and high-altitude sites in North India. J. Geophys. Res.: Atmos. 112, D21307.
Saleh, R., Robinson, E.S., Tkacik, D.S., Ahern, A.T., Liu, S., Aiken, A.C., Sullivan, R.C., Presto, A.A., Dubey, M.K., Yokelson, R.J., Donahue, N.M., Robinson, A.L., 2014. Brownness of organics in aerosols from biomass burning linked to their black carbon content. Nat. Geosci. 7, 647.
Satish, R., Shamjad, P., Thamban, N., Tripathi, S., Rastogi, N., 2017. Temporal characteristics of brown carbon over the central Indo-Gangetic Plain. Environ. Sci. Technol. 51, 6765–6772.
Schmid, O., Artaxo, P., Arnott, W.P., Chand, D., Gatti, L.V., Frank, G.P., Hoffer, A., Schnaiter, M., Andreae, M.O., 2006. Spectral light absorption by ambient aerosols influenced by biomass burning in the Amazon Basin. I: comparison and field calibration of absorption measurement techniques. Atmos. Chem. Phys. 6, 3443–3462.
Schwarz, J.P., Gao, R.S., Spackman, J.R., Watts, L.A., Thomson, D.S., Fahey, D.W., Ryerson, T.B., Peischl, J., Holloway, J.S., Trainer, M., Frost, G.J., Baynard, T., Lack, D.A., de Gouw, J.A., Warneke, C., Del Negro, L.A., 2008. Measurement of the mixing state, mass, and optical size of individual black carbon particles in urban and biomass burning emissions. Geophys. Res. Lett. 35, L13810.
Shamjad, P.M., Tripathi, S.N., Thamban, N.M., Vreeland, H., 2016. Refractive index and absorption attribution of highly absorbing brown carbon aerosols from an urban Indian city-Kanpur. Sci. Rep. 6, 37735.
Singh, A., Rajput, P., Sharma, D., Sarin, M.M., Singh, D., 2014. Black carbon and elemental carbon from postharvest agricultural-waste burning emissions in the Indo-Gangetic Plain. Adv. Meteorol. 2014, 10.
Singh, D.K., Gupta, T., 2015. Speciation of atmospheric polycyclic aromatic hydrocarbons (PAHs) present during fog time collected submicron particles. Environ. Sci. Pollut. Res. http://dx.doi.org/10.1007/s11356-11015-14413-y.
Singh, D.K., Gupta, T., 2016. Role of transition metals with water soluble organic carbon in the formation of secondary organic aerosol and metallo-organics in PM_1 sampled during post monsoon and pre-winter time. J. Aerosol Sci. 94, 56–69.
Srinivas, B., Rastogi, N., Sarin, M.M., Singh, A., Singh, D., 2016. Mass absorption efficiency of light absorbing organic aerosols from source region of paddy-residue burning emissions in the Indo-Gangetic Plain. Atmos. Environ. 125, 360–370.
Srinivas, B., Sarin, M.M., 2014. Brown carbon in atmospheric outflow from the Indo-Gangetic Plain: mass absorption efficiency and temporal variability. Atmos. Environ. 89, 835–843.
UKMO, 1994. Handbook of Aviation Meteorology. United Kingdom Meteorological Organisation (ukmo).
Vaishya, A., Singh, P., Rastogi, S., Babu, S.S., 2017. Aerosol black carbon quantification in the central Indo-Gangetic Plain: seasonal heterogeneity and source apportionment. Atmos. Res. 185, 13–21.
Vautard, R., Yiou, P., van Oldenborgh, G.J., 2009. Decline of fog, mist and haze in Europe over the past 30 years. Nat. Geosci. 2, 115.
Venkataraman, C., Habib, G., Eiguren-Fernandez, A., Miguel, A.H., Friedlander, S.K., 2005. Residential biofuels in South Asia: carbonaceous aerosol emissions and climate impacts. Science 307, 1454–1456.
Weingartner, E., Saathoff, H., Schnaiter, M., Streit, N., Bitnar, B., Baltensperger, U., 2003. Absorption of light by soot particles: determination of the absorption coefficient by means of aethalometers. J. Aerosol Sci. 34, 1445–1463.
WMO, 2005. World Meteorological Organisation. pp. 782. http://trove.nla.gov.au/version/23700569.
Wu, D., 2006. A discussion on difference between haze and fog in city. Meteorology 32, 9–15 (in Chinese).
Zhang, X., Lin, Y.-H., Surratt, J.D., Weber, R.J., 2013. Sources, composition and absorption Ångström exponent of light-absorbing organic components in aerosol extracts from the Los Angeles Basin. Environ. Sci. Technol. 47, 3685–3693.
Zheng, G., He, K., Duan, F., Cheng, Y., Ma, Y., 2013. Measurement of humic-like substances in aerosols: a review. Environ. Pollut. 181, 301–314.